Carbohydrate Polymers **12** (1990) 39–59

The Determination of the Molecular Weight Distribution of Pectins by Calibrated GPC Part I. Calibration by Light Scattering and Membrane Osmometry

G. Berth,[a] H. Dautzenberg,[b] D. Lexow[a] & G. Rother[b]

[a]Central Institute of Nutrition, GDR Academy of Sciences, Arthur-Scheunert-Allee 114–116, Bergholz-Rehbrücke, 1505, GDR
[b]Institute of Polymer Chemistry, GDR Academy of Sciences, Teltow-Seehof, GDR

(Received 15 October 1988; revised version received 8 January 1989; accepted 15 January 1989)

ABSTRACT

Commercial high methoxyl citrus pectin was fractionated on Sepharose 2 B/Sepharose 4 B. Fractions were used to calibrate GPC by light scattering and membrane osmometry. The angular dependence of light scattering of the fractions was interpreted in terms of a two-component system giving reliable $\overline{M}_w/\overline{M}_n$ ratios for the major molecularly dispersed component which forms coils of considerable stiffness in solution. A minor particulate spherical component was identified which was rich in neutral sugars. Structural parameters of this component were determined by comparison of the experimental scattering behavior with master curves. β-Elimination of the fully esterified pectin was carried out to reveal the chemical nature of the particulate component.

INTRODUCTION

Different elution profiles of a series of pectin samples under identical GPC conditions have been often used to attribute differences in some pectin properties to differences in their molecular weights (Beach *et al.*, 1986) or to discuss changes by enzymatic and/or chemical degradations (Thibault, 1983; Michel *et al.*, 1985; Ngyen *et al.*, 1985; Rombouts & Thibault, 1986). In order to convert an elution profile into a molecular weight distribution (MWD) curve, a calibration of GPC is necessary. Since well-characterized standards for pectins are not available, Deckers

Carbohydrate Polymers 0144-8617/89/$03.50

et al. (1986) proposed an HPLC procedure using monodisperse pullulanans and polydisperse pectin samples.

Rapid progress in the field of polysaccharide characterization has been achieved by coupling GPC with a low-angle laser light scattering (LALLS) detector. The idea is to measure directly the MWD of a polymer. The theoretical background is described by Yu and Rollings (1987). Also in pectin studies the coupling of GPC with light scattering detection has been used. Whereas Hourdet and Muller (1987) employed a commercial LALLS equipment in our previous investigations we preferred wide-angle measurements (Anger & Berth, 1986).

This contribution deals with this problem using a commercial high-methoxyl citrus pectin. The task involves pectin characterization by light scattering which has not been solved sufficiently up to now using unfractionated fruit pectins. Light scattering regularly gives weight average molecular weights $\bar{M}_w$ of several millions (Smith, 1976; Berth *et al.*, 1977, 1982; Chapman *et al.*, 1987). They can be considerably reduced by centrifugation (Berth *et al.*, 1977; Kawabata & Sawayama, 1977; Jordan & Brant, 1978; Plashchina *et al.*, 1985; Axelos *et al.*, 1987; Sawayama *et al.*, 1988), but even then they exceed comparable $\bar{M}_w$ values from sedimentation analysis (Säverborn, 1945; Devine, 1974). The latter are far more consistent with number average values $\bar{M}_n$ in the range of 40 000 to 80 000 determined by membrane osmometry (Owens *et al.*, 1946; Glikman & Orlow, 1950; Pals & Hermans, 1952; Devine, 1974; Fritsche *et al.*, 1977; Berth *et al.*, 1980). Thus light scattering should not be considered to be a reliable method of molecular weight determination for pectins without special care (Panchev *et al.*, 1988). As already pointed out (Berth *et al.*, 1977; Berth, 1988) high molecular weight pectin molecules, rich in neutral sugars, play an important role in light scattering measurements but they have only weak effects on intrinsic viscosity $[\eta]$ and $\bar{M}_n$.

It has been accepted now that neutral sugar side chains are highly branched and concentrated on only a small percent of the uronic acid residues, giving 'hairy regions', whereas the major parts of the pectin molecules are present as homogalacturonans giving 'smooth regions' (De Vries *et al.*, 1982, 1986). According to De Vries (1985) commercial fruit pectins consist of a homogalacturonan and a rhamnogalacturonan with side chains of arabinogalactans, apart from minor amounts of xylogalacturonans. By β-elimination with subsequent GPC the 'hairy regions' could be separated (De Vries *et al.*, 1983; Thibault, 1983; Rombouts & Thibault, 1986) since all esterified galacturonans were degraded to small fragments.

Together with the chemical heterogeneity a heterogeneity in architecture was observed (Berth, 1988). A combination of techniques are required to adequately describe a complex polymer of this type.

In this contribution, GPC on Sepharose 2 B/Sepharose 4 B is used for pectin fractionation. The fractions are studied by light scattering, capillary viscosimetry, and membrane osmometry. Light scattering measurements are focused on the angular dependence, and only in some cases are concentration dependencies and Zimm plots (Zimm, 1948) discussed. β-Elimination is used to explain the light scattering behavior. Information on the neutral sugar/galacturonic acid ratios within the fractions is obtained as E_q value derived from the UV spectra of sulphuric acid solutions. In order to interpret the angular dependencies in terms of structural parameters the experimental curves are compared with master curves (Dautzenberg & Rother, 1988). Membrane osmometry is used to determine $\bar{M}_n$ values in order to estimate the heterogeneity $\bar{M}_w/\bar{M}_n$. Radii of gyration calculated according to the Flory theory are compared with those from light scattering. Finally the problems of MWD determination are briefly discussed.

EXPERIMENTAL

Citrus pectin (Koch Light, UK) with a degree of esterification of about 60 to 70% and a galacturonan content of about 70 to 75% was used as the source material. Neutral sugar contents were analyzed by gas chromatography using TMS derivatives after acid hydrolysis. The yield from 10 mg of pectin was 0·37 mg arabinose, 0·88 mg galactose, 0·71 mg glucose, and 0·10 mg rhamnose.

GPC was performed on Sepharose 2 B/Sepharose 4 B with a 0·037 M phosphate buffer of pH 6·5 as eluent. Details are given elsewhere (Berth, 1988). The pectin concentration was monitored continuously using a differential refractometer (Knauer, FRG). The carbohydrate recoveries were about 90%, expressed as galacturonan after calibration with galacturonic acid (Serva, FRG). Fractions (10 ml) were collected to determine the intrinsic viscosities $[\eta]$ at $25{\cdot}00 \pm 0{\cdot}01$°C (Viscomatic, Fica, France) and the molecular weights by light scattering. The photometer Sofica (Fica, France) was equipped with a helium-neon laser (Zeiss Jena, GDR) of wavelength 632 nm. Prior to the light scattering measurements the fractions passed through a membrane filter of pore size 0·45 μm (Sartorius-GmbH, FRG). For each GPC run only one filter was used, and the fractions passed through it in the direction of decreasing number of

fraction. All excess scattering values R_θ are related to the blank eluent which had passed through the membrane first.

To obtain a sufficient quantity for subsequent measurements (osmometry, light scattering, Fig. 6) two neighboring fractions were combined and the corresponding fractions from several GPC runs were collected. After lyophilization the samples were redissolved in distilled water, desalted by repeatedly passing through a column of about 120 ml Epidex B-2 (MLW, GDR) with water as eluent, and lyophilized again.

All symbols in connection with light scattering have their usual meaning (Huglin, 1972). This also covers calculations of $\bar{M}_w$, z-average of R_G and second virial coefficients A_2 calculated from Zimm plots of $K.c/R_\theta$ against $\sin^2(\theta/2)+kc$. To calculate the optical constant K the following values were used: $n_0 = 1{\cdot}334$, $\partial n/\partial c = 0{\cdot}150$ ml g^{-1}, $N_L = 6{\cdot}023 \times 10^{23}$ mol^{-1} and $R_B = 12{\cdot}0 \times 10^{-6}$ cm^{-1} (Millaud & Strazielle, 1979). Using the Guinier plot $\ln(R_\theta/K.c)$ against $\sin^2(\theta/2)$ ln $\bar{M}_w$ was taken from the intercept with the ordinate at zero angle (Kerker, 1969). R_G was derived from

$$P(\theta)_{\theta \to 0} = \exp(-h^2 R_G^2/3) \quad 5 \text{ with}$$

$$R_G^2 = \frac{3|A|}{(4\pi/\lambda)^2}$$

where A is the initial slope.

To compare the experimental scattering curves with master curves light scattering intensities were measured at 31 fixed angles between 30 and 150°.

The E_q values were derived from the UV spectra, at 315 and 297 nm, of the carbohydrate solutions after addition of concentrated sulphuric acid. Details of the determination are given elsewhere (Berth, 1988). Prior to β-elimination 60 mg of the pectin was fully esterified using a solution of diazomethane in ether (Berth *et al.*, 1980). The air-dried pectin was dissolved in 20 ml phosphate buffer (see above) and stored for 4 h at 80°C. After cooling to room temperature 15 ml of this solution were used for GPC.

For osmometry the samples were dissolved at room temperature using the same phosphate buffer. In some cases the solutions were dialyzed against the buffer to remove residual buffer salt. All measurements were carried out at 37°C in 3 or more pectin concentrations (c). The instrument (Knauer, FRG) was equipped with a membrane of type SM 115 39 (Sartorius-GmbH, FRG). $\bar{M}_n$ was calculated in the customary manner (Stuart, 1953) according to

$$\bar{M}_n = \frac{R.T}{(\pi/c)_{c=0} \cdot \rho}$$

where R = universal gas constant, T = temperature in °K, π = osmotic pressure expressed by cm water column, and ρ = density of the solution.

RESULTS AND DISCUSSION

Experimental results

Following previous studies Fig. 1 shows the elution profile of citrus pectin on Sepharose 2 B/Sepharose 4 B together with the E_q values to describe the galacturonic acid/neutral sugar ratio. The shaded area describes the distribution of the compact pectin of high molecular weight and rich in neutral sugars within the eluent (Berth, 1988). The angular dependence of the scattered light is plotted according to Zimm in Fig. 2 for the fractions related to Fig. 1. By reason of the low concentrations given by GPC no dilution or extrapolation to zero concentration was carried out. The derived molecular weights $\bar{M}_w$ and radii of gyration R_G are listed in Table 1 together with the respective intrinsic viscosities $[\eta]$ and number average molecular weights $\bar{M}_n$ by membrane

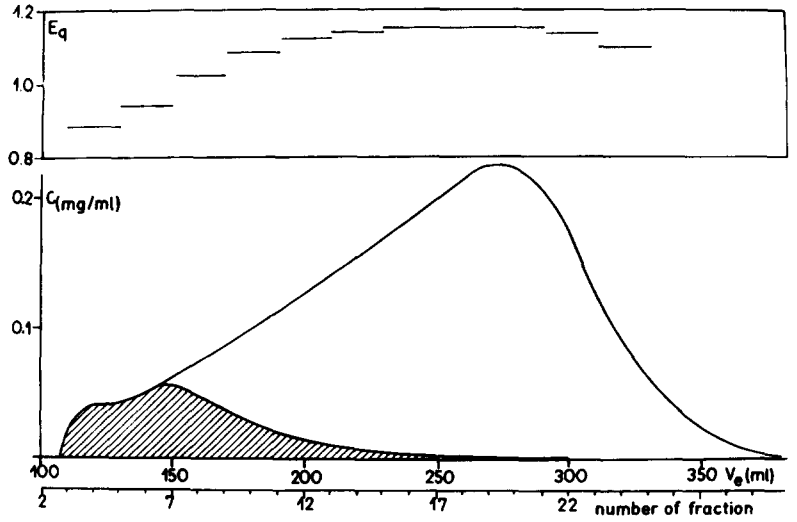

Fig. 1. Elution profile of citrus pectin, E_q values of the fractions and the distribution of compact pectin molecules (shaded).

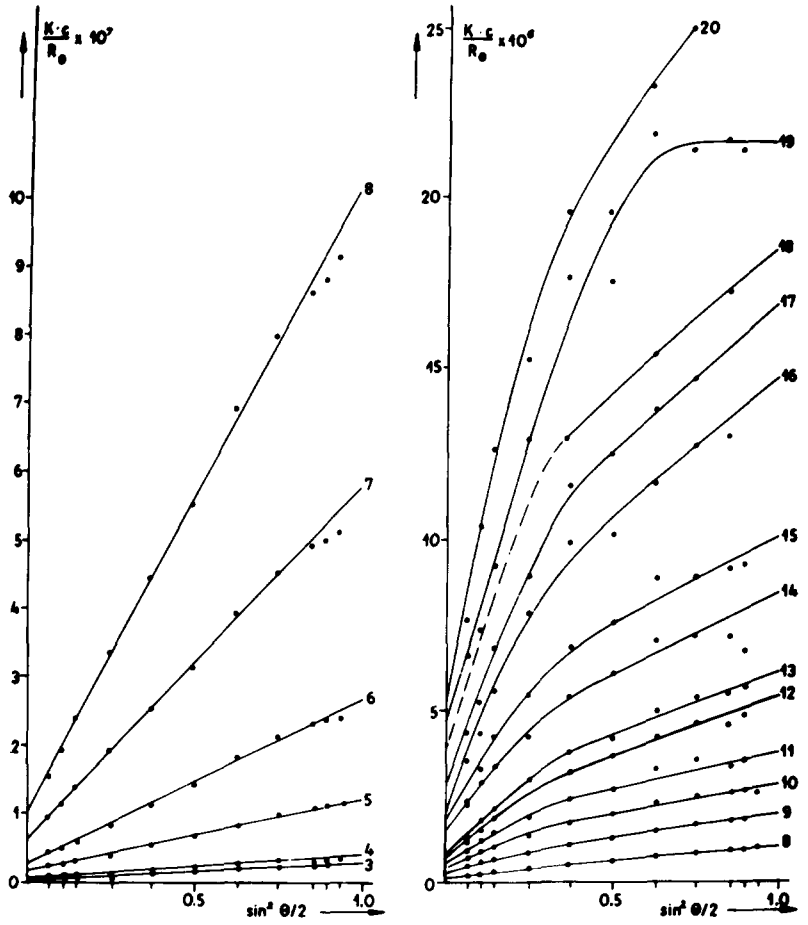

Fig. 2. Zimm plot of the angular dependence of the scattered light of the fractions according to Fig. 1.

osmometry. $\overline{M}_w/\overline{M}_n$ ratios are added. An example of a complete Zimm plot using the fraction 7/8 is given in Fig. 3 to illustrate the characteristic shape for the fractions 3 to 8.

An assessment of all these data will easily reveal their inconsistency. Points to be criticized are as follows: Firstly, the $\overline{M}_w/\overline{M}_n$ ratios are too high to be accepted without doubt for GPC fractions of a series of homologous polymers. Moreover molecular weights $\overline{M}_w$ by sedimentation analysis on comparable pectin fractions were observed to be much lower (Harding & Berth, 1989) with $\overline{M}_w/\overline{M}_n$ ratios of about 1·2, and thus suggesting that the $\overline{M}_n$ values are far better than $\overline{M}_w$ from light scattering. Secondly, both the continuously decreasing $\overline{M}_w$ with increasing elution volume V_e at nearly unchanged R_G values and the course of

TABLE 1
Molecular Weights $\bar{M}_w$ and Radii of Gyration R_G by Light Scattering, Intrinsic Viscosities $[\eta]$ and Molecular Weights $\bar{M}_n$ by Membrane Osmometry

Number of fraction	*Elution volume (ml)*	$[\eta]$ *(ml g^{-1})*	$\bar{M}_w \times 10^{-6}$	R_G *(nm)*	$\bar{M}_n$	$\bar{M}_w/\bar{M}_n$
3	110	112·2	200	—		
4	120	240·0	100	109		
5	130	346·7	66·7	173		
6	140	638·3	40·0	202		
7	150	732·8	16·7	188		
8	160	803·5	10·0	197		
9	170	822·2	5·00	182		
10	180	798·0	2·86	170		
11	190	785·2	2·08	168	121 300	15·5
12	200	724·4	1·667	173		
13	210	636·1	1·351	162	63 630	17·5
14	220	613·8	0·714	149		
15	230	530·9	0·571	152	60 830	8·9
16	240	431·5	0·512	160		
17	250	367·3	0·363	153	39 860	—
18	260	316·2	—	—		
19	270	234·4	0·222	133	27 000	8·0
20	280	199·5	0·208	150		
21	290	169·8	—	—	20 350	
22	300	147·9	—	—		
23	310	118·9	—	—	15 720	
24	320	86·1	—	—		

$[\eta]$ with V_e are not consistent with a polymer fractionation according to hydrodynamic volume. Thirdly, the strong angular dependence of the scattered light even at fractions with relatively low molecular weights does not agree with general experience for other polymer systems.

It is a disadvantage of the Zimm procedure that the product of $\bar{M}_w$ and the scattering function $P(\theta)$ is plotted against $\sin^2(\theta/2)$. Consequently the scattering curves are flattening with steadily increasing molecular weight. Using a Guinier plot,

$$\ln \frac{R_\theta}{K.c} = \ln \bar{M}_w + \ln P(\theta)$$

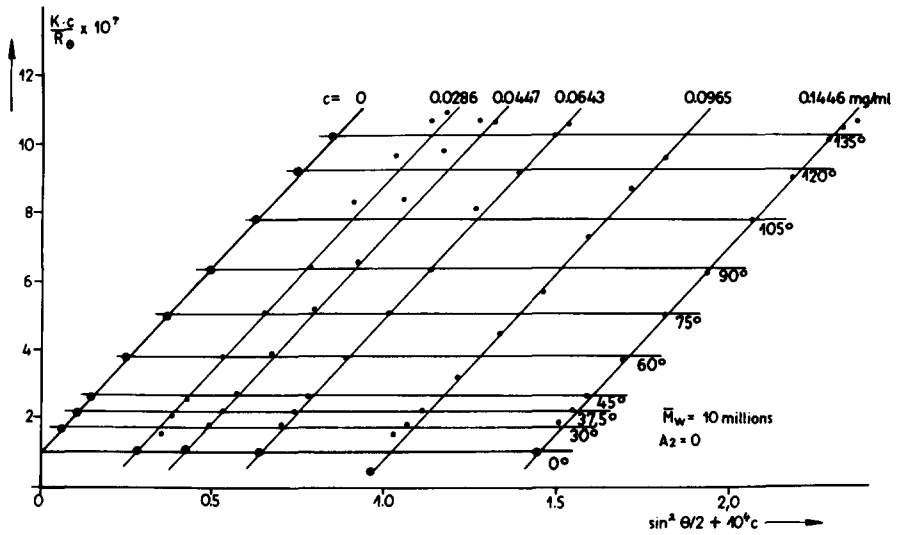

Fig. 3. Zimm plot of the fraction 7/8.

both quantities have been decoupled so that the scattering function, independent of all changes in V_e and $\bar{M}_w$, can be immediately observed. This is shown in Fig. 4. All values of $\bar{M}_w$ or R_G derived from Fig. 4 do not differ markedly from those in Table 1. The tendency of $P(\theta)$ to change steadily, as seen by the strongly curved lines within the whole angular range up to 50° and then the steadily flattening character above 50°, is obvious. The curved low-angle range below 50°C remains nearly unchanged for all the fractions. This may indicate bimodal systems of altering heterogeneity, confirming previous results. The strong increase of the scattering intensity within the low-angle range is likely to be due to small amounts of very large particles, whereas the major component of molecularly dispersed pectin mainly determines the wide-angle range. The very similar curvature within the low-angle range suggests a nearly identical particle component of the same size level in all fractions. A formal interpretation of the scattering curves as a one-component system does not give relevant information concerning both parts of the mixture. Therefore we shall give an interpretation in terms of a two-component system.

Interpretation of the light scattering data in terms of a two-component system

It was the aim to separate the scattering curves into the contributions of both components in order to achieve their individual characterization. As

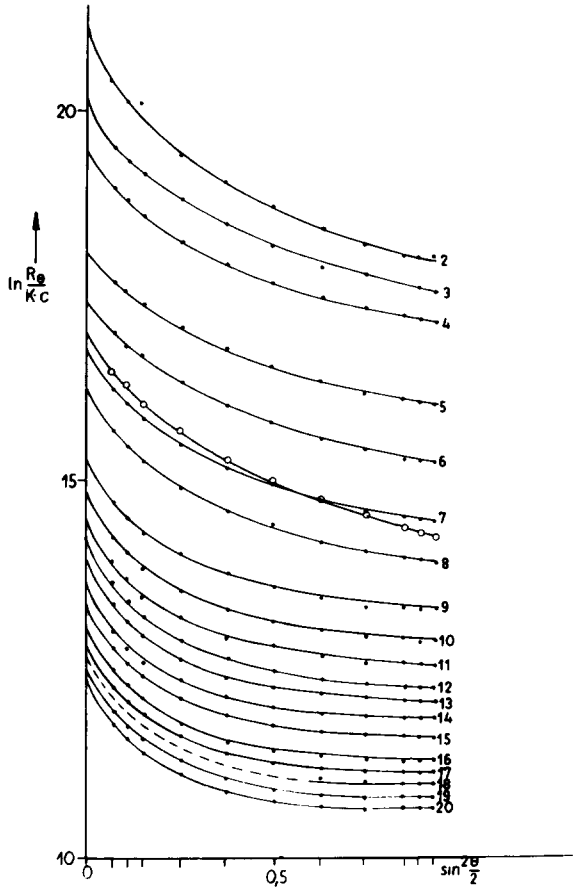

Fig. 4. Guinier plot of the angular dependence of the scattered light of the fractions according to Fig. 1; ○ — original citrus pectin (0·1% solution).

a criterion for the separation it was assumed that osmometry has given the true molecular weights of the molecularly dispersed pectin. Even if we take into account a molecular weight distribution within the GPC fractions no angular dependence of the scattering curves is expected for molecules with $\overline{M}_n$ values given in Table 1. To eliminate the contribution of the particulate component we used the following algorithm: Fraction 3 was assumed as representative for the particulate component. The scattering curve of fraction 3 was multiplied by a factor $k_i'(k_i' < 1)$ and then subtracted from scattering of the fractions $i = 7, \ldots, 20$ by varying k_i' until the condition of angular independence required above had been fulfilled.

Characterization of the molecularly dispersed component

Figure 5 illustrates the good quality of the results obtained. Molecular weights derived are listed in Table 2 together with the k_i' values and the normalized k_i value which are related to unit concentration. The $\bar{M}_w/\bar{M}_n$ ratios are now much more normal than before (Table 1) for GPC fractions. The physical meaning of the k_i values is that they are a measure of the mass contribution of the particulate component, implying again that fraction 3 exclusively consists of this component. It amounts to less than 1% in fraction 8 and decrease steadily to extremely small concentrations, but even then strongly affecting the low-angle light scattering behavior.

To remove these traces and then confirm the calculated $\bar{M}_w$ in Table 2 experimentally six isolated pectin fractions prepared with the same GPC equipment were filtered through membrane filters of pore size 0·1 μm. The filtration steps were repeated until rather constant scattering intensities were achieved. The results are shown in Fig. 6. They justify the interpretation of the scattering curves above. Therefore after the preparative removal of the particulate traces, light scattering measurements at only one angle, e.g. 90°, are sufficient to determine $\bar{M}_w$ and A_2. Results obtained are summarized in Table 3. Our A_2 values exceed those reported by Plashchina *et al.* (1985) which is likely to be due to the larger heterogeneities for their samples. The high loss on filtration (particularly for fractions 13/14 and 15/16) indicates that an additional fractionation of the molecularly dispersed pectin cannot be avoided. This is also re-

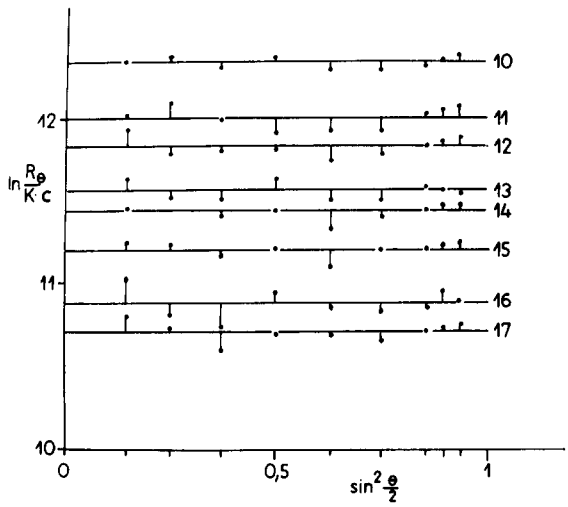

Fig. 5. Calculated scattering curves of the molecularly dispersed pectin component in GPC fractions.

TABLE 2

Molecular Weights $\bar{M}_w$, k_i' and Normalized k_i Values (see the text), and Radii of Gyration $R_{[\eta]}$ According to the Flory Theory

Number of fraction	k_i	$\bar{M}_w \times 10^{-5}$	k_i	$R_{[\eta]}$ *(nm)*
7	$3{\cdot}39 \times 10^{-2}$	6·06	$1{\cdot}98 \times 10^{-2}$	60
8	$1{\cdot}95 \times 10^{-2}$	3·29	$0{\cdot}94 \times 10^{-2}$	51
9	$7{\cdot}00 \times 10^{-3}$	2·78	$2{\cdot}87 \times 10^{-3}$	48
10	$3{\cdot}87 \times 10^{-3}$	2·29	$1{\cdot}38 \times 10^{-3}$	45
11	$2{\cdot}71 \times 10^{-3}$	1·63	$8{\cdot}65 \times 10^{-4}$	40
12	$1{\cdot}90 \times 10^{-3}$	1·37	$5{\cdot}38 \times 10^{-4}$	37
13	$1{\cdot}75 \times 10^{-3}$	1·07	$4{\cdot}49 \times 10^{-4}$	32
14	$1{\cdot}00 \times 10^{-3}$	0·94	$2{\cdot}39 \times 10^{-4}$	31
15	$7{\cdot}92 \times 10^{-4}$	0·74	$1{\cdot}71 \times 10^{-4}$	27
16	$5{\cdot}69 \times 10^{-4}$	0·53	$1{\cdot}12 \times 10^{-4}$	23
17	$4{\cdot}85 \times 10^{-4}$	0·45	$8{\cdot}68 \times 10^{-5}$	20
18	$3{\cdot}85 \times 10^{-4}$	0·42	$6{\cdot}33 \times 10^{-5}$	19
19	$3{\cdot}44 \times 10^{-4}$	0·29	$5{\cdot}49 \times 10^{-5}$	15
20	$2{\cdot}59 \times 10^{-4}$	0·28	$4{\cdot}19 \times 10^{-5}$	14

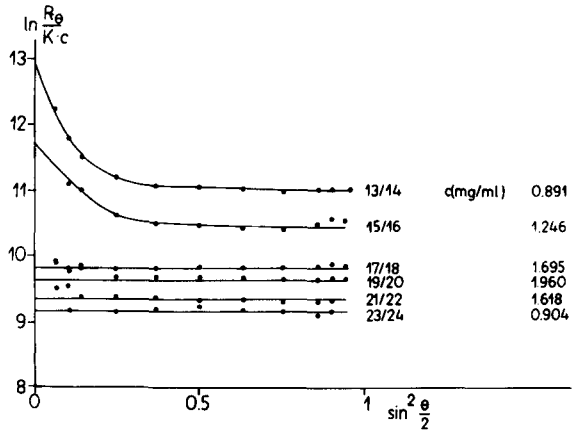

Fig. 6. Experimental scattering curves of GPC fractions after filtration through membrane filters of pore size 0·1 μm.

flected by the molecular weights in Fig. 7 which were found to be too low.

This figure collects all the molecular weights above by plotting their logarithm against the elution volume. It demonstrates obviously that apart from the Zimm interpretation of the light scattering all data are

TABLE 3
Molecular Weights $\bar{M}_w$ and Second Virial Coefficients A_2 by Light Scattering and Loss of Pectin after Filtration Through 0·1 μm Pore Size Membranes

Number of fraction	$\bar{M}_w$	$A_2 \times 10^2$	*Loss after filtration (%)*	$\bar{M}_w/\bar{M}_n$[a]
13/14	62 500	(0)[b]	12	0·98
15/16	52 350	(0·4)[b]	9	0·86
17/18	45 450	(0·9)[b]	2	1·14
19/20	31 750	0·8	~0	1·18
21/22	22 200	1·3	0	1·09
23/24	16 650	2·4	0	1·06

[a] $\bar{M}_n$ see Table 1 without filtration.
[b] Only apparent values because of the fractionation at filtration.

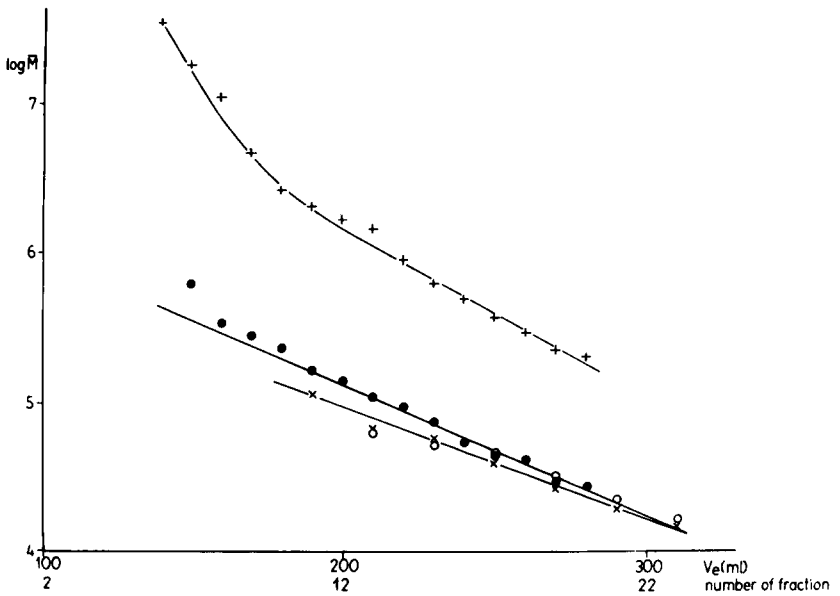

Fig. 7. Calibration line log $\bar{M}$ against the elution volume V_e. +, $\bar{M}_w$ by light scattering interpreted as one-component system; ●, $\bar{M}_w$ of the molecularly dispersed pectin by light scattering interpreted in terms of a two-component system; ○, $\bar{M}_w$ after filtration through membrane filters of pore size 0·1 μm; ×, $\bar{M}_n$ by membrane osmometry.

consistent with each other giving a well-established calibration line. This calibration line in connection with the elution profile permits one to derive the MWD curve (Fig. 8) of the pectin studied. The value $\bar{M}_n = 44\,600$ of the original pectin is in good agreement with this MWD curve. In this plot the heterogeneity of the pectin fractions was ignored

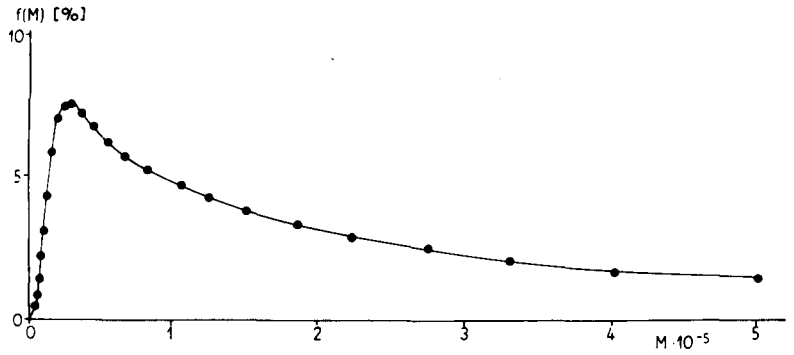

Fig. 8. Molecular weight distribution of this h.m. citrus pectin without respect to its heterogeneity.

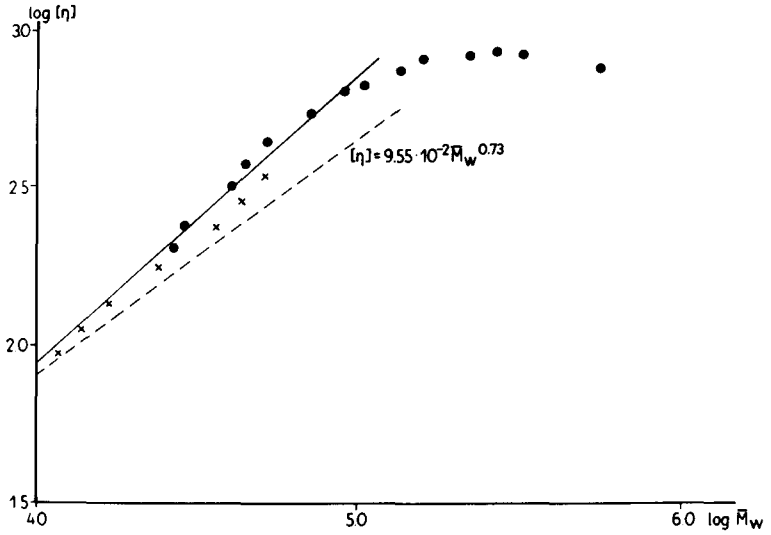

Fig. 9. Mark-Houwink plot. ●, $[\eta]$ from Table 1, $\bar{M}_w$ from Table 2; ×, $[\eta]$ and $\bar{M}_w$ after filtration through membranes of pore size 0·1 μm. From Anger and Berth (1986).

taking into account all carbohydrate under the elution line and using a calibration straight line which holds only for molecularly dispersed pectin. This point will be discussed in a further paper. The compromise above is chosen in favor of the major component.

According to our explanation light scattering alone does not allow one to determine either the dimension or the shape of the pectin molecules forming the major fraction. Information about the shape is obtained from the Mark-Houwink plot in Fig. 9. The slope of the straight line section of log $[\eta]$ against log $\bar{M}_w$ with $\alpha = 0{\cdot}89$ is a characteristic feature of linear polymers with stiff chains forming coil-shaped structures. This slope is

higher than reported previously (Anger & Berth, 1986) because the interpretation of light scattering as a two-component system reduces the molecular weights due to the slight but measurable contribution of the particulate component in the wide-angle range. The curvature at molecular weights above 10^5 does not vanish, indicating a molecularly dispersed branched pectin fraction.

Based on this concept $R_{[\eta]}$ values (Table 2) were calculated according to Flory's theory

$$(\overline{h^2})^{3/2} = \frac{[\eta].M}{\phi_\varepsilon}$$

where

$$\overline{R^2_{[\eta]}} = \overline{h^2}/6$$

and

$$\phi = \phi_0(1 - 2{\cdot}63\varepsilon + 2{\cdot}86\varepsilon^2)$$

with

$$\varepsilon = \tfrac{2}{3}(\alpha - 0{\cdot}5) \text{ and } \phi_0 = 2{\cdot}68 \times 10^{23}$$

despite the deviation from θ conditions.

This treatment can only cover the region of proportionality between $\log[\eta]$ and $\log \bar{M}_w$, and it provides values which are much smaller than those in Table 1.

The polymer homologous series described here is likely to be identical with the homogalacturonan fraction of De Vries.

Characterization of the particulate component

Structural parameters. Now we will focus on the particulate component. The separation of the scattering curves into two parts was carried out assuming that the particulate component can be described by the scattering curve of fraction 3. Therefore more detailed information about changes of the structural parameters with the number of the fraction is not available on this basis, but the mass fraction of the particulate component can be estimated (see the values of k_i in Table 2). These results show that only traces of the particulate component are present in the low molecular weight fractions.

To get information about the structural parameters of the particulate component, we measured the scattering intensity at 31 angular positions and analyzed the scattering curves in more detail. For the interpretation

of the scattering curves a recently developed method (Dautzenberg & Rother, 1988) was used, based on a comparison of the experimental curves with theoretically calculated master curves. For computation of the theoretical curves a special logarithmic distribution function (Hartmann & Dautzenberg, 1983) was used, which separates the influence of the size parameter a_m and the polydispersity σ. In the framework of the Rayleigh-Debye-approximation the size parameter a_m generally occurs in the scattering functions as a product with the scattering parameter $h(h = 4\pi/\lambda . \sin \theta/2)$. Therefore the a_m-dependence of the scattering curves may be represented by a single curve. In a double logarithmic plot $\log R_\theta/K.c$ versus $\log (a_m . h)$ a variation of a_m corresponds only to parallel shifts along the x-axis. Consequently the two-dimensional dependence on a_m and σ is reduced to a set of scattering curves with different values of σ. Such master curves were calculated for spheres of homogeneous density, and Gaussian coils (Dautzenberg & Rother, 1988).

For sufficiently large particles ($a_m > 100$ nm) the experimental curve can be assigned in many cases to a master curve in an unambiguous manner and for spheres the polydispersity of the scattering system can also be assessed. Placing the experimental scattering curve on the theoretical one yields M_w and a_m, and from these parameters we obtain the polymer packing density in the particles by the simple relation $M_w = 4\pi/3\rho . N_A . a_m^3$ (N_A — Avogadro's number).

In Fig. 10 the scattering curves of the original sample and of the fractions 3/4, 5/6, 7/8 and 13/14 are given as master plots. The similarity of all the curves justified the choice of the scattering curve of fraction 3 for the separation procedure. The experimental values correspond to the crosses, while the full lines represent the sections of appropriate theoretical scattering curves of polydisperse systems of spheres with particle parameters given in Table 4. The agreement between the experimental points and the theoretical curves is excellent. An assignment of the experimental curves to scattering curves of Gaussian coils leads to differences in the scattering intensities of about 50%. Consequently the analysis of the scattering curves confirms the compact structure of the particles. Information about the anisometry of the particles cannot be obtained, because, e.g. the scattering of a monodisperse system of ellipsoids of revolution corresponds to the scattering of a polydisperse system of spheres. Nevertheless the determination of the particle parameters by master curves allows very small changes in the particulate component to be detected.

In Table 4 the particle parameters of the investigated samples are listed. It must be mentioned that only the product of the mass fraction of

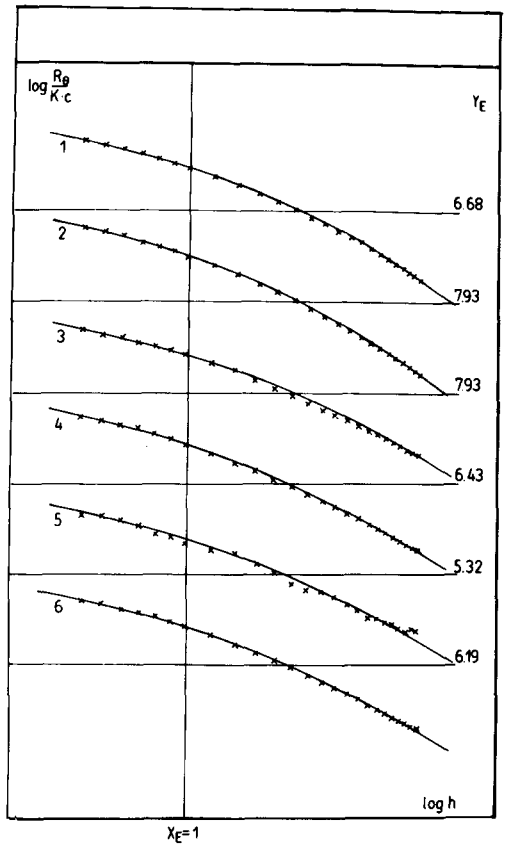

Fig. 10. Experimental scattering curves and master plot for: 1, original sample; 2, fraction 3/4; 3, fraction 5/6; 4, fraction 7/8; 5, fraction 13/14; 6, original sample after esterification and β-elimination.

TABLE 4
Structural Parameter of the Particulate Component

Sample	σ	a_m *(nm)*	a_{max} *(nm)*	$x_p \cdot M_w$	$x_p \cdot \rho$ *(g ml^{-1})*	x_p *($\rho = 0{\cdot}1$ g ml^{-1})*
Original sample	0·6	122	50	$2{\cdot}2 \times 10^7$	$4{\cdot}8 \times 10^{-3}$	0·05
Fraction 3/4	0·6	132	54	$4{\cdot}5 \times 10^8$	$7{\cdot}8 \times 10^{-2}$	1
Fraction 5/6	0·7	106	31	$3{\cdot}7 \times 10^8$	$1{\cdot}2 \times 10^{-1}$	1
Fraction 7/8	0·7	107	34	$1{\cdot}3 \times 10^7$	$3{\cdot}2 \times 10^{-3}$	0·03
Fraction 13/14	0·7	112	33	$9{\cdot}3 \times 10^5$	$2{\cdot}6 \times 10^{-4}$	0·003
Original sample after β-elimination[a]	0·7	112	33	$7{\cdot}4 \times 10^6$	$2{\cdot}1 \times 10^{-3}$	0·02

[a]See next section.

the particle component x_p and M_w of the particles and also the product $x_p \cdot \rho$ can be determined, because in the data evaluation as concentration the total polymer concentration was used.

Assuming that the fractions 3/4 and 5/6 consist predominantly of particles ($x_p = 1$), we obtain for the polymer packing density $\rho = 0{\cdot}1$ g ml^{-1}. Using this value the mass fraction of the particulate component in the other samples may be estimated (see last column in Table 4). The original sample contains only 5% particles. The amount of particles in a fraction decreases drastically with increasing function number: in the fractions 13/14 only 0·3% of the polymer is present as particles.

The values obtained for the particle radii show that no remarkable differences could be observed. However the slight decrease of a_m from fraction 3/4 to 5/6 indicates some fractionation by GPC.

This effect is not so clearly expressed in the case of lower molecular fractions, because they contain only very small amounts of particles. The polydispersity of the systems increases slightly in the direction of low molecular fractions. The radius a_m derived from light scattering data is correlated with the size in the maximum of the distribution function by the relation $a_{max} = \exp(-\frac{5}{2}\sigma^2)\, a_m$. The values of a_{max} are also given in Table 4.

Chemical composition. In order to identify the chemical nature of the particulate component the original pectin sample was fully esterified (degree of esterification about 95% without changes of the elution profile compared with the original one) and then degraded by β-elimination. This was accompanied with a decrease of $[\eta]$ to about 20 ml g^{-1} instead of 345 ml g^{-1} initially thus indicating a complete degradation of the molecularly dispersed homogalacturonan fraction to low-molecular weight fragments. The scattering intensities of a 0·1% (w/v) solution were diminished to about a quarter due to β-elimination, indicating a partial degradation of strongly scattering material. This was accompanied by a slight increase of σ and a decrease in the particulate component of 2% instead of 5% before (Table 4).

Since the glucose found could result from starch or its high molecular constituents, β-elimination was carried out in the presence of α-amylase BAN 240 (Novo, Denmark) at 70°C and pH 6·5. Thereby the scattering level was diminished slightly but the shape of the curve maintained. The reaction with iodine did not give unequivocal results. Thus traces of starch cannot be excluded but do not explain the scattering behavior observed.

The elution profile is shown in Fig. 11. Similar to other authors' results (De Vries *et al.*, 1983; Thibault, 1983; Rombouts & Thibault,

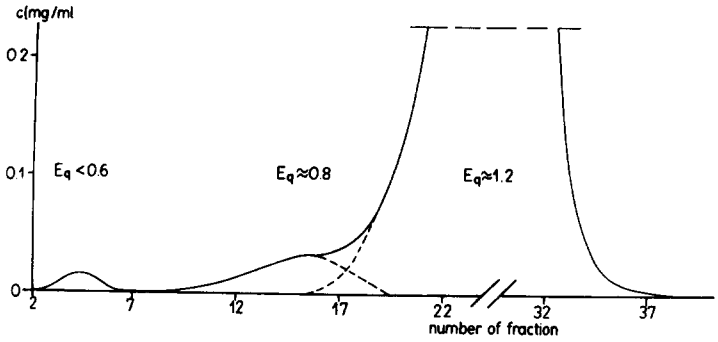

Fig. 11. Elution pattern of the fully esterified citrus pectin after β-elimination and E_q values of some fractions.

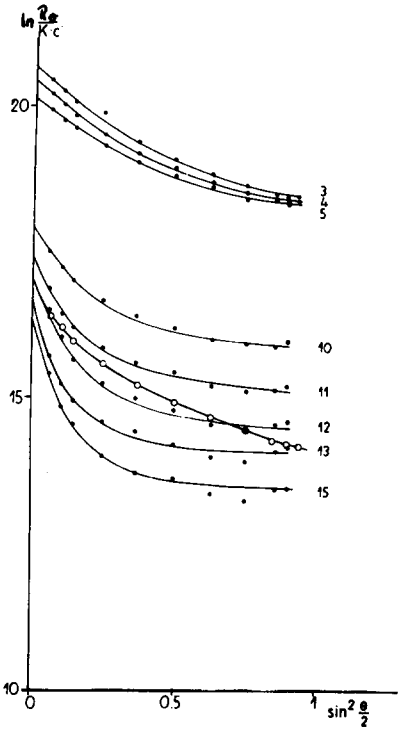

Fig. 12. Guinier plot of the angular dependence of the scattered light of the fractions according to Fig. 11; o — original citrus pectin (0·1% solution).

1986) the peak at the void volume with $E_q < 0{\cdot}6$ consists of relatively pure neutral sugar polymers whereas the next peak with $E_q \sim 0{\cdot}8$ contains markedly galacturonic acid residues. Both peaks added up are equal to 5% of the total carbohydrate. The scattering curves of these fractions are given in Fig. 12. Obviously the shape of curve 3 coincides

nearly with the scattering curve of the original pectin and with the first two GPC fractions of the original pectin.

All these curves are only shifted along the ordinate depending on the mass ratio of this component. These findings show that even traces of this extremely high molecular weight material decisively influence light scattering measurements. The decreasing initial slope of the scattering curves 3 to 5 in Fig. 12 also demonstrates that the light scattering technique is even sensitive enough to detect the fractionation of this material within the fractions 3 to 5. The scattering curves 10 to 15 are not discussed in detail. They suggest that the fractions consist of a high molecular weight and polydisperse material which was fractionated according to the molecular weight, and also a minor part with very high molecular weights.

It should be mentioned that the first 12 fractions from Fig. 1 after esterification and β-elimination yield the same fragmentation pattern in GPC, but with different proportions of the two neutral sugar peaks (Berth, unpublished).

Proposal for the structure. Considering

- the reduction of the light scattering intensity due to β-elimination, which is slight in comparison with the reduction of $[\eta]$,
- the distribution of neutral sugars within the eluent before and after β-elimination,
- the fragmentation patterns of the fractions, and the original pectin both before and after esterification and subsequent β-elimination,

our results suggest that the particulate component is a heterogenous material composed of molecules which differ in chemical composition and structure. The minor part eluted at the void volume before and after β-elimination represents extremely high molecular weight particles, with high polymer densities and spherical shape, consisting of highly branched neutral sugars without internal galacturonic acid blocks. Therefore it cannot be degraded by β-elimination. Probably shorter galacturonan regions occur on the outside and have little effect on the viscosity but guarantee the polyelectrolyte character during ion exchange chromatography (Berth, 1988). Their influence on the intrinsic viscosity of the unfractionated sample is only slight (Table 1).

The major part as an intermediate between molecularly dispersed branched pectins and non-degradable spheres consists of reduced neutral sugar regions alternating with galacturonan regions thus realizing together with the branched molecularly dispersed species the middle peak with $E_q \sim 0{\cdot}8$ after β-elimination and the variety of rich in neutral

sugars polymers in the original population. Consequently the molecules are more compact than a homogalacturonan, which is consistent with the flattening of the $\log[\eta] - \log \bar{M}_w$ curve.

This corresponds to De Vries' conception of 'hairy and smooth regions'. Based on the results of the β-elimination we agree with his model where the differences between molecules are due to the number of 'hairy regions' linked with each other by 'smooth regions'.

ACKNOWLEDGEMENTS

The authors thank Mrs K. Schaller and Mrs S. Brandt for careful assistance. The neutral sugar analysis was performed by Dr M. Petrzika at the Central Institute of Nutrition, Bergholz-Rehbrücke.

REFERENCES

Anger, H. & Berth, G. (1986). *Carbohydr. Polym.*, **6**, 193.

Axelos, M. A. V., Lefebvre, J. & Thibault, J. F. (1987). *Food Hydrocolloids*, **1**, 569.

Beach, P., Davis, E., Ikkala, P. & Lunbye, M. (1986). In *Chemistry and Function of Pectins*, ed. M. C. Fishman & J. J. Len. ACS Symposium Series 310.

Berth, G. (1988). *Carbohydr. Polym.*, **8**, 105.

Berth, G., unpublished.

Berth, G., Anger, H. & Linow, F. (1977). *Nahrung*, **21**, 939.

Berth, G., Anger, H. & Lexow, D. (1980). *Nahrung*, **24**, 529.

Berth, G., Anger, H., Plashchina, I. G., Braudo, E. E. & Tolstogusov, V. B. (1982). *Carbohydr. Polym.*, **2**, 1.

Chapman, H. D., Morris, V. J., Selvendran, R. R. & O'Neill, M. A. (1987). *Carbohydr. Res.*, **165**, 53.

Dautzenberg, H. & Rother, G. (1988). *J. Polym. Sci., Part B, Polymer Physics*, **26**, 353.

Deckers, H. A., Olieman, C., Rombouts, F. M. & Pilnik, W. (1986). *Carbohydr. Polym.*, **6**, 361.

Devine, W. C. (1974). *Physico-chemical studies on pectins.* PhD Thesis, University of Edinburgh.

De Vries, J. A. (1985). *Gums and Stabilizers for the Food Industry.* The Third International Conference and Industrial Exhibition, Wrexham, UK.

De Vries, J. A., Rombouts, F. M., Voragen, A. G. J. & Pilnik, W. (1982). *Carbohydr. Polym.*, **2**, 25.

De Vries, J. A., den Uijl, C. H., Voragen, A. G. J., Rombouts, F. M. & Pilnik, W. (1983). *Carbohydr. Polym.*, **3**, 193.

De Vries, J. A., Voragen, A. G. J., Rombouts, F. M. & Pilnik, W. (1986). In *Chemistry and Function of Pectins*, ed. M. C. Fishman & J. J. Len. ACS Symposium Series 310.

Fritsche, P., Lehmann, J., Dongowski, G. & Bock, W. (1977). *Faserforsch. u. Textiltechn.*, **28**, 543.
Glikman, S. A. & Orlow, S. I. (1950). *Izv. Akad. Nauk SSSR, Khim. Ser.*, **71**, 895.
Harding, S. E. & Berth, G. (1989). Unpublished.
Hartmann, M. & Dautzenberg, H. (1983). *Acta Polymerica*, **34**, 52.
Hourdet, D. & Muller, G. (1987). *Carbohydr. Polym.*, **7**, 301.
Huglin, M. B. (ed.) (1972). *Light Scattering on Polymer Solutions.* Academic Press, London and New York.
Jordan, R. C. & Brant, D. A. (1978). *Biopolymers*, **17**, 2885.
Kawabata, A. & Sawayama, S. (1977). *Nippon Nogeikagaku Kaishi*, **51**, 15.
Kerker, M. (1969). *The Scattering of Light and Other Electro-Magnetic Radiation.* Academic Press, New York, San Francisco, London.
Michel, F., Thibault, J. F., Mercier, C., Heitz, F. L. & Pouillaude, F. (1985). *J. Food Sci.*, **50**, 1499.
Millaud, B. & Strazielle, C. (1979). *Makromol. Chem.*, **180**, 441.
Ngyen-The, C., Soty, M. & Breuils, L. (1985). *Sci. Aliments*, **5**, 639.
Owens, H. S., Lotzkar, H., Schultz, T. M. & Naclay, W. D. (1946). *J. Amer. Chem. Soc.*, **68**, 1628.
Pals, D. T. F. & Hermans, J. J. (1952). *Recueil Trav. Chim. Pays-Bas*, **71**, 458.
Panchev, I. N., Kirtchev, N. A., Kratchanov, C. G. & Proichev, T. (1988). *Carbohydr. Polym.*, **8**, 257.
Plashchina, I. G., Semenova, M. G., Braudo, E. E. & Tolstogusov, V. B. (1985). *Carbohydr. Polym.*, **5**, 159.
Rombouts, F. M. & Thibault, J. F. (1986). *Carbohydr. Res.*, **154**, 189.
Säverborn, S. (1945). *A Contribution to the Knowledge of the Acid Polyuronides.* Almquist and Wiksells, Uppsala, Sweden.
Sawayama, S., Kawabata, A., Nakahara, H. & Kamata, T. (1988). *Food Hydrocolloids*, **2**, 31.
Smith, J. E. (1976). *The Molecular Weights of Pectins.* PhD Thesis, University of Leeds.
Stuart, H. A. (ed.) (1953). *Die Physik der Hochpolymeren.* Springer-Verlag Berlin, Göttingen, Heidelberg.
Thibault, J. F. (1983). *Phytochemistry*, **22**, 1567.
Yu, Li Ping & Rollings, J. E. (1987). *J. Appl. Polym. Sci.*, **33**, 1909.
Zimm, B. H. (1948). *J. Chem. Phys.*, **16**, 1093, 1099.